



# Near-Surface Azimuthal Magnetic Fields and Their Role in Solar Activity Cycles

Andrey G. Tlatov<sup>1</sup>

Received: 16 September 2023 / Accepted: 13 December 2023 / Published online: 22 December 2023  
© The Author(s), under exclusive licence to Springer Nature B.V. 2023

## Abstract

We consider variations of the azimuthal magnetic fields of the Sun in the 23–25 activity cycles according to observations with SDO/HMI, SOHO/MDI, and Kislovodsk/STOP telescopes. To identify azimuthal magnetic fields, the daily observations of LOS magnetic fields from the regions near the solar limb were analyzed. It is shown that with a sufficiently large averaging of the data, large-scale structures are distinguished, which can be interpreted by horizontal magnetic fields along the east–west direction. Azimuthal magnetic fields are visible at both low and high latitudes. Azimuthal fields at the same latitudes have opposite directions in the northern and southern hemispheres and also change sign in even and odd cycles of activity.

The mechanism of formation of global azimuthal magnetic fields and their role in the cycle of solar activity is discussed. The near-surface azimuthal magnetic field is closely related to the activity cycle. Apparently, the azimuthal field is formed from U-shaped flux tubes of active regions (AR). Due to the presence of the tilt angle AR during differential rotation, the subsurface magnetic fields are pulled in the azimuthal direction. The role of azimuthal magnetic fields in solar activity cycles is considered. A scheme for the generation of a magnetic field different from Babcock–Leighton dynamo models is proposed.

**Keywords** Solar cycle · Magnetic field · Solar activities

## 1. Introduction

Solar cycle manifests itself as an ordered process of excitation and dissipation of the magnetic field. There are general patterns in this process that manifest in different cycles and at different latitudes. For example, Spoerer’s law, Hale’s law of sunspot polarity, Maunder’s butterfly diagram, or the regular reversal of the magnetic field in polar regions. These patterns are valid for both hemispheres of the Sun and can be traced throughout many cycles of activity. Such an organization of magnetic activity involves the formation of large-scale or global magnetic fields.

---

✉ A.G. Tlatov  
[tlatov@mail.ru](mailto:tlatov@mail.ru)

<sup>1</sup> Kislovodsk Mountain Astronomical Station of the Pulkovo Observatory, Gagarina str. 100, Kislovodsk, 357700, Russia

Solar activity is a consequence of the inductive action of fluid flows on large-scale magnetic fields (Charbonneau, 2020). The solar photospheric magnetic flux is formed by the rise of toroidal magnetic fields from the depth of the Sun in the form of active regions (AR), mainly in the form of bipolar structures. The total magnetic flux of each individual AR is approximately zero. However, observations show (Babcock, 1959) that unipolar large-scale magnetic fields of different polarities are formed in different hemispheres as the activity cycle at high latitudes develops. The global magnetic field is most well manifested in the minima of solar activity, when the large-scale magnetic field takes configurations close to the dipole.

The polar fields of the Sun, located at the heliographic poles of the Sun, have a large-scale unipolar distribution covering a range of latitudes from about  $\pm 50^\circ - 60^\circ$  during most phases of the solar cycle, except for the period they change magnetic polarity. It is believed that their magnetic configuration is relatively simple, with predominantly almost vertical magnetic-field lines (Petrie, 2023).

However, the question about the existence of horizontal magnetic fields remains open. (Tsuneta et al., 2008; Petrie, 2023). This is partly due to the difficulty of observing horizontal magnetic fields on the Sun. There are local horizontal magnetic fields associated with local sources, such as magnetic loops (Pastor Yabar, Martínez-González, and Collados, 2018). But so far, there is insufficient evidence for the existence of long-lived large-scale horizontal fields. Such fields can play a particularly important role in high-latitude regions, where they affect the formation of the coronal magnetic field on a large spatial scale, as well as because of their role in the solar-activity cycle (Petrie, 2015).

Liu and Scherrer (2022) obtained the distribution of toroidal fields using the method of measuring the difference of magnetic fields on the eastern and western limbs (Duvall et al., 1979). Based on the observations of WSO, MDI, and HMI magnetograms, they were able to detect a picture of an extended activity cycle lasting approximately 16.8 years.

In this paper, the observations of LOS magnetograms are analyzed, but the main attention is paid to the allocation of horizontal large-scale magnetic fields. The analysis of the sources of possible azimuthal fields is carried out. Based on the observational data, a mechanism for the formation of a near-surface magnetic field and the formation of sources for generating the next activity cycle is proposed.

## 2. Identification of Azimuthal Magnetic Fields

Direct measurements of horizontal magnetic fields can be performed by observing the full magnetic-field vector on the photosphere. At the same time, there are difficulties in registering and interpreting the signal of the transverse component of the field (Petrie, 2023). The sensitivity of magnetographs for transverse fields with Zeeman effect is usually an order of magnitude lower than for longitudinal signals. The Zeeman effect for linear polarization is proportional to the square of the transverse field strength and therefore weaker than the Zeeman effect for circular polarization, which has a linear dependence on the longitudinal field strength. Because of this quadratic dependence, the orientation of the transverse field suffers from the so-called 180-degree azimuth ambiguity, which must be resolved.

Since the observation of horizontal magnetic fields is difficult, we will use the observation data of the longitudinal component of the magnetic field. We will consider areas near the solar limb where the azimuthal component of the magnetic field can be seen at a small angle. To better determine the azimuthal component, we can consider the difference in the intensity of magnetic fields near the eastern (E) and western limbs (W). The main data used in this

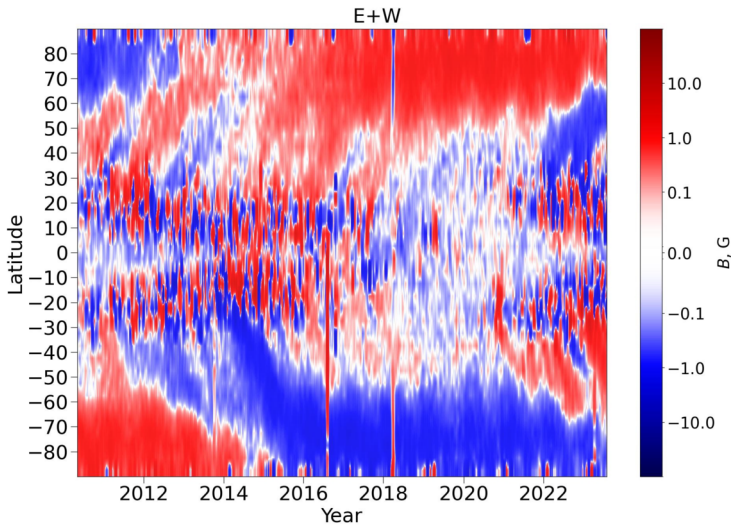


**Figure 1** Measurements of the magnetic field near the limb of the Sun according to SDO/HMI data. The sum of the magnetic-field intensities at the eastern and western limb is presented ( $B_E + B_W$ ).

work were the magnetic-field data gathered with the *Solar Dynamics Observatory/Helioseismic and Magnetic Imager* (SDO/HMI). To reduce noise, in the period 2010–2023, we processed five images for each day at times close to 00:00, 05:00, 10:00, 15:00, and 20:00 UT. The regions separated from the central meridian by  $\phi = 70^\circ - 85^\circ$  in longitude and  $5^\circ$  wide in latitude near the E and W limbs were measured. For each day of observations, by averaging 5 observations at different points in time, we calculated the average values separately for the eastern  $B_E$  and western  $B_W$  limbs. To plot the graphs, we used a logarithmic scale of magnetic-field intensity for the eastern  $B_E$  and western  $B_W$  limbs, taking into account the sign of the magnetic field, which improved the contrast of the diagrams for fields of different intensities.

Figure 1 shows the distribution in latitude-time coordinates for the sum of the values of  $B_E + B_W$ . The distribution is close to the distribution for magnetic fields when sampling near the central meridian, although with different amplitudes of magnetic fields, since strong magnetic fields, for example in the sunspots umbra, the magnetic field is mainly vertical. The region where AR exists in the form of sunspot “butterflies” and unipolar regions at high latitudes are visible. This diagram shows that the formation of polar regions occurs during the drift of fields with a polarity corresponding to the magnetic polarity of the trailing sunspots in the form of flux pulses.

Figure 2 shows a diagram of the magnetic-field difference ( $B_E - B_W$ ). To reduce noise, daily values in each latitude interval were smoothed by a sliding window of 27 days. The distribution in Figure 2 in comparison with Figure 1 has changed significantly. We see large areas of fields of the same sign changing with the solar cycle. The distribution is asymmetric in the hemispheres. In the region of the formation of sunspots, we see unipolar regions. Latitudinal drift of regions of the same sign is observed during the activity cycle from the middle latitudes to the equator.

We also see an ordered structure of the assumed azimuthal magnetic field at high latitudes. Comparing Figures 1 and 2, we see that azimuthal magnetic fields of Cycle 25 appeared at latitudes  $r \approx 50^\circ - 60^\circ$  in 2015–2016, that is, several years before the appearance

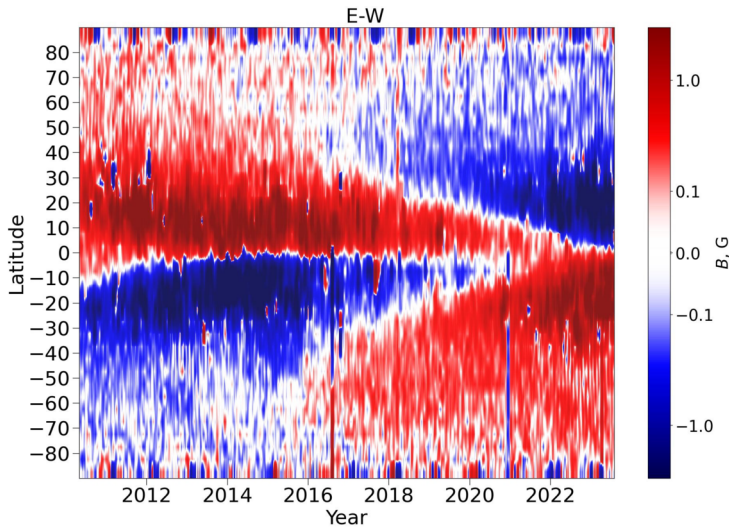


**Figure 2** The difference in magnetic-field measurements at the eastern and western limb ( $B_E - B_W$ ) according to SDO/HMI data.

of sunspots of Cycle 25. Azimuthal fields of Cycle 24 near the equator disappear in the period 2020–2022. We can assume that the duration of the existence of azimuthal fields in the cycle of activity is  $r \approx 16$ –18 years, which is similar to the hypothesis of an extended activity cycle. This result is close to analysis Liu and Scherrer (2022).

At high latitudes, azimuthal magnetic fields drift to the poles, which may be due to a transfer with meridional circulation. At the same time, we do not observe any drift of the flux pulses from the sunspot zone to the poles, as in Figure 1. It is possible that azimuthal magnetic fields have a significantly longer formation time and are more resistant to solar-activity-pulses.

Figures 3 and 4 show separately the values of  $B_E$  and  $B_W$ , respectively. At latitudes above  $50^\circ$ , both on the eastern limb and on the western limb, we observe regions with the same magnetic polarity. The sign of the magnetic field  $B_E$  and  $B_W$  at high latitudes coincides with the sign of the magnetic fields for sunspots with trailing polarity in activity cycles. But at latitudes below  $30^\circ$ , the magnetic field polarities on the eastern and western limbs (Figures 3 and 4) have opposite signs. In addition, the sign of polarity on each hemisphere changes with a new activity cycle. In the active latitudes, fields with trailing sunspot polarity dominate the eastern limb in each hemisphere (Figure 3), whereas fields with leading polarity dominate the western limb (Figure 4). This polarity distribution corresponds to the direction of the magnetic field in coronal loops over the active regions.

The structure of the polarity distribution of magnetic fields near the limb is also confirmed by the data from other magnetographs. For these purposes, we used the observation data of the SOHO/MDI magnetograph in the period 1996–2011 and the STOP magnetograph in Kislovodsk 2014–2023. As well as for the analysis of SDO/HMI data for SOHO/MDI data, we used several observations per day. Figure 5 shows the intensity distribution diagrams on the eastern  $B_E$  and western  $B_W$  limbs according to the SOHO/MDI magnetograph data. As well as for the SDO/HMI data in the low-latitude zone, the polarity of  $B_E$  and  $B_W$  has the opposite sign on the eastern and western limbs. After 2004, strong annual variations are

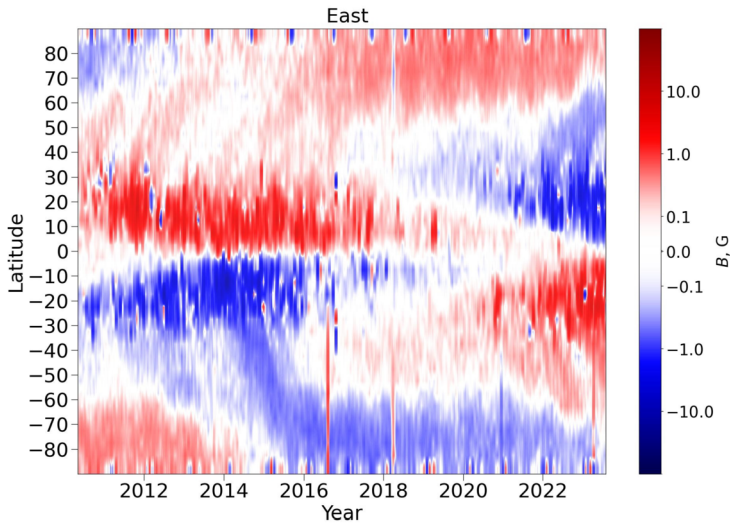


**Figure 3** Diagram of the distribution of the magnetic field near the eastern limb  $B_E$  according to SDO/HMI data.

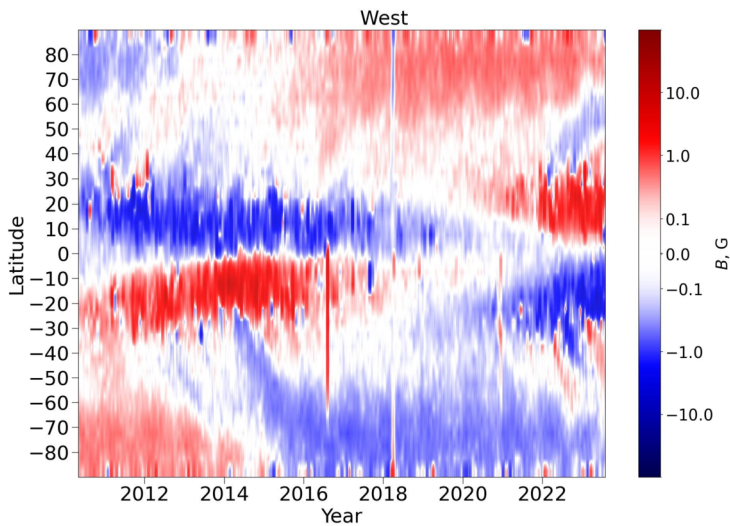


**Figure 4** Diagram of the distribution of the magnetic field near the western limb  $B_W$  according to SDO/HMI data.

visible, probably related to the noise component in the SOHO/MDI observations (Liu and Scherrer, 2022).

To exclude the possibility of an error in the recovery of magnetic fields from the observational data of the spectra in the left and right circular polarization, we performed an analysis of the observational data of the magnetograph large-scale magnetic field STOP installed at the Kislovodsk Mountain Astronomical Station (KMAS). Unlike the SDO/HMI and SOHO/MDI filter magnetographs, the STOP magnetograph is made according to the

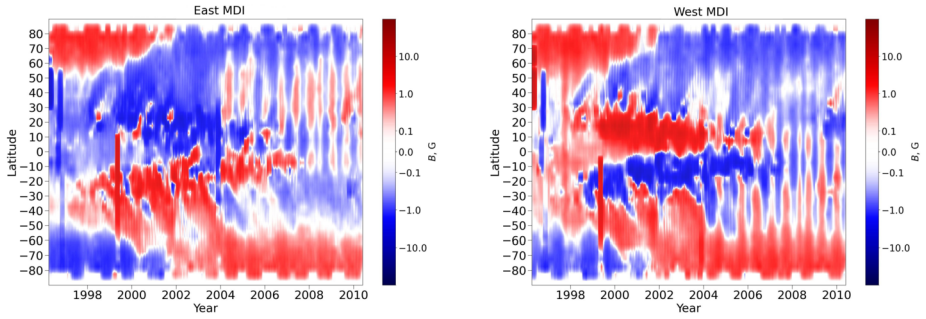


**Figure 5** Diagram of the magnetic-field intensity distribution near the eastern limb  $B_E$  (left) and the western limb  $B_W$  (right) according to SOHO/MDI data.

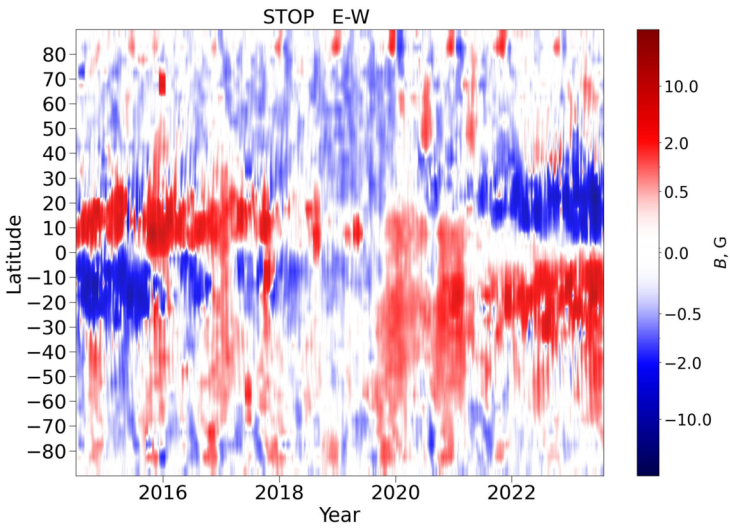


**Figure 6** The difference in the intensity of the magnetic fields ( $B_E - B_W$ ) according to the observations of the magnetograph STOP.

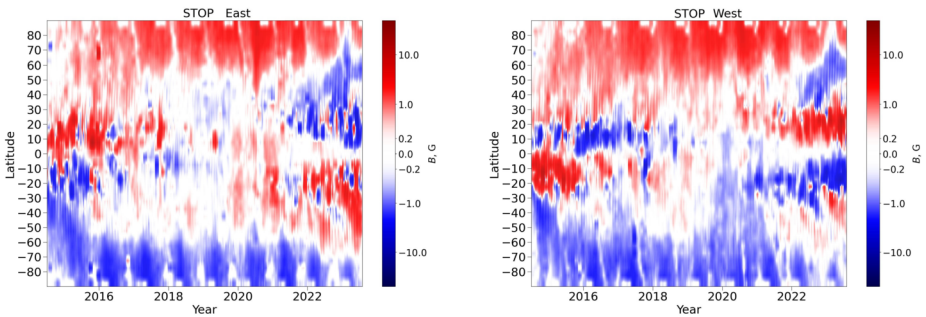


**Figure 7** Diagram of the magnetic-field intensity distribution near the eastern limb  $B_E$  (left) and the western limb  $B_W$  (right) according to STOP data.

spectrogeiograph scheme (Tlatov et al., 2015). To restore magnetic fields, an original technique based on the analysis of spectral line profiles in left and right circular polarization is used. STOP observational data are available since 2014 to date (Tlatov and Berezin, 2023).

Figure 6 shows the intensity difference on the eastern and western limbs of  $B_E - B_W$ , and Figure 7 shows the intensity separately on the western and eastern limbs according to STOP data. The main large-scale structures correspond to Figures 2, 3, and 4.

### 3. Possible Sources of Azimuthal Magnetic Field

In the diagrams of Figures 3, 4, 6, and 7, we see that in the sunspot zone, the intensity of the magnetic field changes its sign depending on the limb at which the measurements were carried out. This may indicate the presence of an azimuthal magnetic field. However, it can also be caused by other processes. One of the mechanisms may be the influence of the rotation of the Sun on the measurement of magnetic fields. Indeed, the direction of the radial velocity on the eastern and western limbs is opposite. However, there are objections to this explanation. We see the change of polarity only in the sunspot zone and not in high latitudes, although the rotation should have affected different latitudinal zones. Secondly, we have used our original technique in restoring the magnetic field according to the STOP magnetograph data. This technique is based on the analysis of the full profile of spectral lines of left and right circular polarization. At the same time, the constant component of the signal associated with rotation was subtracted. Therefore, the rotation of the Sun cannot explain the observed imbalance.

It is possible that the east-west difference appears only in sunspots or active areas. For example, due to the Evershed (Evershed, 1909) and Wilson (Wilson and Maskelyne, 1774) effects. Indeed, in the penumbra of sunspots, the direction of the magnetic field deviates from the vertical. To verify this, consider the polarity of the magnetic fields in the penumbra of the sunspots near the limb. The technique for distinguishing the boundaries of sunspots and the penumbra of sunspots is described in Tlatov (2022, 2023). Figure 8 shows the polarity diagrams of magnetic fields in the penumbra of sunspots separately for the eastern and western limbs. In contrast to Figures 3, 4, and 7, we see that the polarities of the sunspots in Figure 8 essentially do not change for the east and west. The prevailing polarity of the magnetic field in the diagrams of Figure 8 corresponds to the polarity of the leading sunspots.

It is possible that the distributions in Figures 3, 4, and 7 are not related to sunspots, but to large magnetic structures, such as solar faculae. Faculae can be observed in “white” light, near the limb. We have identified flares in the sunspot formation zone and at high latitudes according to observations in the SDO/HMI continuum. The contours of the faculae were transferred to observations of magnetic fields made at the same time to determine the magnetic field inside them. Figure 9 shows a diagram of the polarity distribution of the magnetic fields of the faculae near the eastern and western limbs. In the mid-latitude zone, we see a distribution with mixed polarity and no unipolar regions. Thus, the magnetic-field polarity distributions in Figures 3, 4, and 7 are not related to the features of magnetic fields in active regions.

Another mechanism for the formation of an east–west asymmetry in the distribution of the polarity of magnetic fields may be differential rotation with depth. In this case, the magnetic fields may deviate from the vertical. However, since such a mechanism acts equally on fields of different polarity, and it is believed that the magnetic flux of solar bipoles is compensated, this mechanism cannot explain the practically unipolar structures on the eastern and western limb. Even if we assume the presence of unbalanced magnetic fields, we would

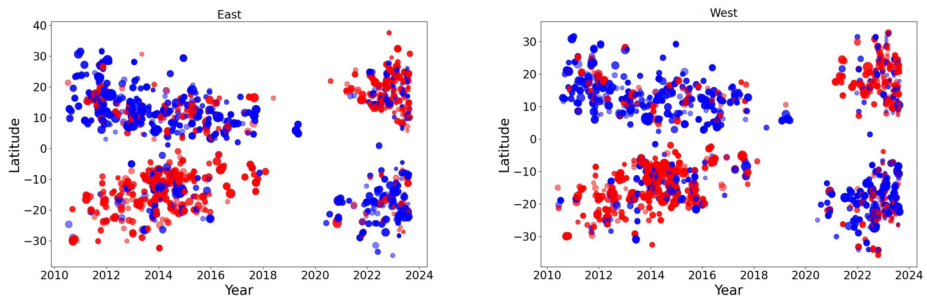


**Figure 8** The distribution of the polarity of magnetic fields in the penumbra of sunspots, measured near the limb  $r/R > 0.9$ . (Left) on the eastern limb. (Right) on the western limb.

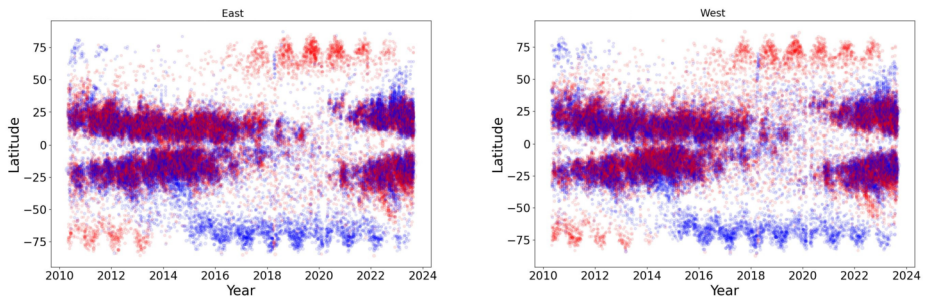


**Figure 9** The polarity distribution of magnetic fields in faculae visible in “white” light according to SDO/HMI data and measured near the limb  $r/R > 0.9$ . (Left) on the eastern limb. (Right) on the western limb.

see significantly different amplitudes at the eastern and western limb. However, we do not see this in Figures 3, 4, and 7. Hence, it is difficult to explain the distributions in Figures 3, 4, and 7 by differential rotation. The main explanation remains the variant with the presence of an azimuthal magnetic field.

#### 4. Formation of a Near-Surface Magnetic Field

From the analysis of daily observations of the longitudinal magnetic fields of the full disk of the Sun, we found a difference in the directions of the magnetic fields at the eastern and western limbs of the Sun. The time-latitude diagram (Figures 2 and 6) shows that the regions of the magnetic-field intensity difference parameter form long-lived large-scale structures, both in the low-latitude and high-latitude regions of the Sun. Perhaps this indicates the existence of a large-scale azimuthal magnetic field. Large-scale azimuthal magnetic fields can complement solar-cycle generation models.

Currently, one of the most popular models is the Babcock–Leighton dynamo (Babcock, 1959; Leighton, 1964). In this model, the toroidal magnetic field from the generation zone emerges due to buoyancy as active regions on the surface of the Sun. Further, the magnetic fields of the trailing parts of the active regions drift to the poles, and the magnetic fields of the parts of the leading polarities of different hemispheres are mutually annihilated through the equator. As a result, a new poloidal magnetic field of the dipole type is created, which sinks



to the generation zone and, together with differential rotation, forms a toroidal magnetic field of a new cycle.

The AR flow occurs in cycles with an average period of  $\approx 11$  years at low latitudes (latitude  $\pm 40^\circ$ ). Further, the magnetic flux is dispersed over the solar surface due to the diffusion effect of convective solar supergranulation flows, as well as differential rotation and meridional circulation (Wang, Nash, and Sheeley, 1989; Charbonneau, 2020).

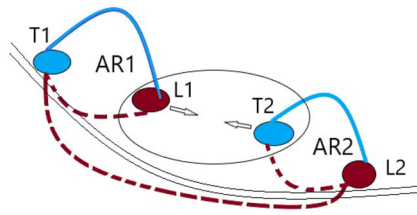
At the same time, it can be seen from observations that the change of the sign of a large-scale magnetic field begins almost immediately after the appearance of a new AR cycle (Figure 1). Sunspots at this moment are located at sufficiently high latitudes,  $\pm 30^\circ$  away from the equator. Therefore, it is not entirely clear how the magnetic fields of the leading polarity of AR can be mutually destroyed through the equator with the fields of the other hemisphere. Thus, the mechanism of formation of a large-scale magnetic field remains not fully understood.

The patterns of the occurrence of flows are the key to the cyclic interaction of AR and polar fields. According to Hale's law of polarity, bipoles in the northern or southern hemisphere of the Sun during a given cycle of activity have a leading/trailing magnetic flux of the same polarity, with opposite polarity in the northern and southern hemispheres. This polarity is reversed in each next cycle. Moreover, the flux of the leading polarity of magnetic bipoles is on average located at a lower latitude than the flux of the trailing polarity. This bias is called Joy's law (Hale et al., 1919). Thus, the bipoles appear to be tilted relative to the equator. Joy's law leads to the fact that the trailing polarity of the bipolar AR dominates at high latitudes.

We can assume that the multiple rising of AR in each hemisphere is important for solar cyclicity, as well as the shift of the average latitude of AR to the equator, called Maunder butterflies and Joy's law. Consider the evolution of active regions. Suppose that the flux tubes of sunspots do not extend far into the convective zone, but form a U-shaped configuration. Since the trailing parts of the AR lie on average higher in latitude than the leading parts, the U-configuration power tube is affected by differential rotation. At the same time, the distance between the geometric centers of the trailing and leading polarities increases with time. That is, the U-tube elongates in the azimuthal direction.

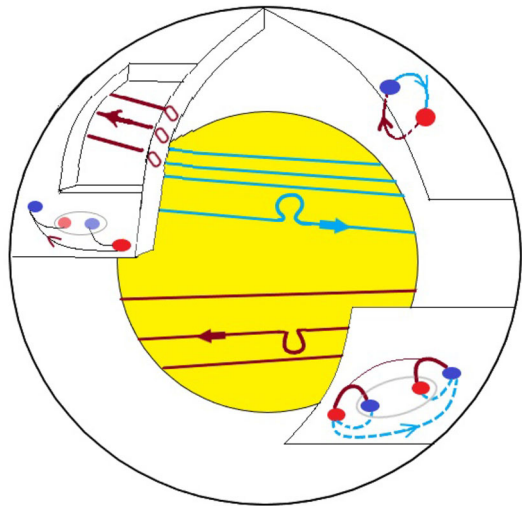
Consider the evolution of two neighboring active regions AR1 and AR2. Due to Maunder's law, the latitude of the area that surfaced later in time (AR2) is on average closer to the equator. And due to Joy's law, the latitudinal distance between the leading sunspot of the first AR1 (L1) and the trailing sunspot of the second AR2 (T2) is on average smaller than between the trailing sunspot of the first AR1 (T1) and the leading sunspot of the second AR2 (L2). This leads to a preferential reconnection of the magnetic fields L1 and T2 and to the formation of a power tube between T1 and L2 (Figure 10). This mechanism creates an azimuthal magnetic field under the photosphere.

Figure 11 shows the distribution scheme of azimuthal magnetic fields in the solar convective zone. During the ascent and interaction of many ARS, azimuthal magnetic fields are formed in each hemisphere under the photosphere. The direction of this azimuthal field under the photosphere to the opposite toroidal magnetic field in the generation zone at the base of the convective zone (Figure 11). Due to the meridional circulation, the new field is transferred to high latitudes and then to the generation zone. In addition to the azimuthal component, due to the geometry of AR, in particular Joy's law, a poloidal magnetic field is also formed. This poloidal magnetic field forms the observed distribution of a large-scale magnetic field at the poles. Also, the poloidal component, when transferred to the generation zone at the base of the convective zone, provides reinforcement of the toroidal component at the base of the convective zone.



**Figure 10** Scheme of the formation of an azimuthal magnetic field under the photosphere. Stretching of the magnetic field tube AR in the azimuthal direction as a result of differential rotation. The interaction of the leading and trailing parts of the two ARs and the formation of a new azimuthal field tube.

**Figure 11** Scheme of the existence of azimuthal magnetic fields in the convective zone of the Sun. There are two areas. One is near the base of the convective zone and the second is under the photosphere near the surface.



The observed azimuthal field (Figures 2 and 6) has a direction corresponding to the direction of the magnetic field of the sunspots with the trailing polarity. In Figure 11, this direction in the northern hemisphere is represented in blue. That is, this sign of the observed azimuthal field (Figures 2 and 6) corresponds to the field above the surface. At the same time, the transfer of the subphotospheric toroidal field is essential for the scheme described above. This is due to the fact that the forming fields of the U-configuration are submerged under the photosphere. The assumed subphotospheric azimuthal field has a direction opposite to the azimuthal field at the base of the convective zone. At the same time, the fields of the upper part of the magnetic field loops will be visible on the photosphere. The immersion of the toroidal field can be caused by the movement of matter in supergranules.

Due to the meridional circulation, the new field is moved to the generation zone. In addition to the azimuthal component, due to the geometry of the AR, a poloidal magnetic field is also formed (Figure 11). This poloidal magnetic field forms the observed distribution of a large-scale magnetic field at the poles. Also, the poloidal component, when transferred to the generation zone, provides strengthening of the toroidal component at the base of the convective zone.

The presented scheme of magnetic-field generation is based on the observed effects, such as Maunder's law, Joy's law, meridional circulation, and differential rotation. This scheme does not require mutual destruction of the fields of the leading regions of the northern and

southern hemispheres across the equator. But there are two zones of formation of toroidal magnetic fields at the base of the convective zone and under the photosphere.

## 5. Conclusion

In this article, the analysis of daily magnetograms according to the data from SDO/HMI, SOHO/MDI, and STOP magnetographs is carried out in order to isolate large-scale horizontal magnetic fields. For this purpose, LOS magnetograms were used and measurements were carried out near the solar limb in the eastern and western hemispheres of the Sun. To distinguish the signal above the noise, several observations per day and time averaging were used. This made it possible to identify long-lived structures that can be interpreted by the existence of a large-scale azimuthal magnetic field  $B_T^P$ .

A scheme for the formation of a near-surface azimuthal field  $B_T^P$  is proposed. Such a magnetic field is formed when the U-shaped tubes of the surfaced active regions are pulled out. The set of surfaced AR forms a single axisymmetric magnetic field having both azimuthal and poloidal components. In favor of this, a quieter change in the azimuthal field (Figure 2) can serve, compared with a more sporadic change in individual components (Figures 3 and 4). Due to the presence of tilt angle AR, differential rotation at the surface stretches the U-structures, strengthening the azimuthal field at the surface.

During the cycle, the new  $B_T^P$  field is transferred to the poles, where the poloidal part is visible as unipolar high-latitude caps of a large-scale magnetic field. The new field is transferred to the generation zone. The transfer can be carried out by conveyor transport by meridional circulation or by other mechanisms of dipping of this field.

The near-surface azimuthal field of the component has the opposite polarity in different hemispheres and changes its sign in successive cycles of activity (Figure 2). The azimuthal field of the current cycle appears at mid-latitudes several years before the start of the sunspot cycle. It is possible that the source of the azimuthal field during this period is ephemeral regions.

**Acknowledgments** Data are courtesy of NASA/SDO and the HMI science team.

**Author contributions** A. T. wrote the manuscript.

**Funding** We acknowledge the financial support the Russian Science Foundation (RSF, project N 23-22-00165).

**Data Availability** All data used are available at the HMI JSOC.

## Declarations

**Competing interests** The authors declare no competing interests.

## References

- Babcock, H.D.: 1959, *Astrophys. J.* **130**, 364. DOI.
- Charbonneau, P.: 2020, *Living Rev. Solar Phys.* **17**, 4. DOI.
- Duvall, T.L.J., Scherrer, P.H., Svalgaard, L., Wilcox, J.M.: 1979, *Solar Phys.* **61**, 233.
- Evershed, J.: 1909, *Mon. Not. Roy. Astron. Soc.* **69**, 454.
- Hale, G.E., Ellerman, F., Nicholson, S.B., Joy, A.H.: 1919, *Astrophys. J.* **49**, 153. DOI.

- Leighton, R.B.: 1964, *Astrophys. J.* **140**, 1547.
- Liu, A.L., Scherrer, P.H.: 2022, *Astrophys. J. Lett.* **927**, L2. DOI.
- Pastor Yabar, A., Martínez-González, M.J., Collados, M.: 2018, *Astron. Astrophys.* **616**, A46. DOI.
- Petrie, G.J.D.: 2015, *Living Rev. Solar Phys.* **12**, 5. DOI.
- Petrie, G.J.D.: 2023, *Solar Phys.* **298**, 43. DOI.
- Tlatov, A.G.: 2022, *Solar Phys.* **297**, 110. DOI.
- Tlatov, A.G.: 2023, *Solar Phys.* **298**, 93. DOI.
- Tlatov, A.G., Berezin, I.A.: 2023, *Geomagn. Aeron.* **63**(8), 70. DOI.
- Tlatov, A.G., Dormidontov, D.V., Kirpichev, R.V., Pashchenko, M.P., Shramko, A.D., Peshcherov, V.S., Grigoryev, V.M., Demidov, M.L., Svidskii, P.M.: 2015, *Geomagn. Aeron.* **55**, 969. DOI.
- Tsuneta, S., Ichimoto, K., Katsukawa, Y., Lites, B.W., Matsuzaki, K., Nagata, S., Orozco Suárez, D., Shimizu, T., Shimojo, M., Shine, R.A., Suematsu, Y., Suzuki, T.K., Tarbell, T.D., Title, A.M.: 2008, *Astrophys. J.* **698**, 1374. DOI.
- Wang, Y.-M., Nash, A.G., Sheeley, N.R. Jr.: 1989, *Astrophys. J.* **298**, 529. DOI.
- Wilson, A., Maskelyne, N.: 1774, *Phil. Trans. Roy. Soc. London* **64**, 1.

**Publisher's Note** Springer Nature remains neutral with regard to jurisdictional claims in published maps and institutional affiliations.

Springer Nature or its licensor (e.g. a society or other partner) holds exclusive rights to this article under a publishing agreement with the author(s) or other rightsholder(s); author self-archiving of the accepted manuscript version of this article is solely governed by the terms of such publishing agreement and applicable law.